Thyroid hormone receptor phosphorylation regulates acute fasting-induced suppression of the hypothalamic–pituitary–thyroid axis

Svetlana Minakhina[a,1], Vanessa De Oliveira[b], Sun Young Kim[a], Haiyan Zheng[c], and Fredric E. Wondisford[a,1]

[a]Department of Medicine, Robert Wood Johnson Medical School, Rutgers, The State University of New Jersey, New Brunswick, NJ 08901; [b]Division of Cancer Biology, Department of Radiation Oncology, Rutgers Cancer Institute of New Jersey, Newark, NJ 007103; and [c]Biological Mass Spectrometry Facility, Robert Wood Johnson Medical School, Rutgers, The State University of New Jersey, Piscataway, NJ 08854

Edited by Mitchell A. Lazar, University of Pennsylvania, Philadelphia, PA, and approved August 23, 2021 (received for review April 27, 2021)

Fasting induces profound changes in the hypothalamic–pituitary–thyroid (HPT) axis. After binding thyroid hormone (TH), the TH receptor beta 2 isoform (THRB2) represses *Trh* and *Tsh* subunit genes and is the principle negative regulator of the HPT axis. Using mass spectrometry, we identified a major phosphorylation site in the AF-1 domain of THRB2 (serine 101, S101), which is conserved among many members of the nuclear hormone receptor superfamily. More than 50% of THRB2 is phosphorylated at S101 in cultured thyrotrophs (TαT1.1) and in the mouse pituitary. All other THR isoforms lack this site and exhibit limited overall levels of phosphorylation. To determine the importance of THRB2 S101 phosphorylation, we used the TαT1.1 cell line and S101A mutant knock-in mice (*Thrb2*^{S101A}). We found that TH promoted S101 THRB2 phosphorylation and was essential for repression of the axis at physiologic TH concentrations. In mice, THRB2 phosphorylation was also increased by fasting and mimicked *Trh* and *Tshb* repression by TH. In vitro studies demonstrated that a master metabolic sensor, AMP-activated kinase (AMPK) induced phosphorylation at the same site and caused *Tshb* repression independent of TH. Furthermore, we identified cyclin-dependent kinase 2 (CDK2) as a direct kinase phosphorylating THRB2 S101 and propose that AMPK or TH increase S101 phosphorylation through the activity of CDK2. This study provides a physiologically relevant function for THR phosphorylation, which permits nutritional deprivation and TH to use a common mechanism for acute suppression of the HPT axis.

hypothalamic–pituitary–thyroid (HPT) | THRB2 | nuclear receptor | phosphorylation | fasting

The thyroid hormones (THs) T_3 and T_4 influence vertebrate development and facilitate metabolic responses to environmental cues such as temperature change, stress, inflammation, and nutrient deficiency (1). TH production in the thyroid gland is regulated by the hypothalamic–pituitary–thyroid (HPT) axis through coordinated release of thyrotropin-releasing hormone (TRH) from the paraventricular nucleus (PVN) of the hypothalamus and thyroid-stimulating hormone (TSH) from anterior pituitary thyrotrophs.

Peripheral and central actions of THs are mediated by three related thyroid hormone receptors (THRA1, THRB1, and THRB2) encoded by two genes (*Thrb* and *Thra*, and for review, see refs. 1 and 2). All isoforms are capable of either activating or repressing target gene expression in a TH-dependent manner (3–5). THRB2 is unique, however, due to its tissue-limited yet robust expression in the anterior pituitary and TRH neurons, where it functions as a potent negative regulator of the *Trh* and *Tsh* subunit genes (5–7).

Similar to the effect of TH, a reduced nutritional status down-regulates the HPT axis both in rodents and in humans (8–12). These changes are presumed to be an adaptive mechanism to conserve energy during times of food shortage. Fasting alters the central HPT axis (reviewed in refs. 1 and 12–14), resulting in reduced levels of TH (especially T_3), which in part is due to a reduction in TRH and TSH levels (11, 15, 16). Prolonged fasting also affects peripheral TH metabolism and cooperatively reduces THs in the circulation (1, 16, 17). However, low serum THs during fasting do not elevate *Trh* and *Tshb* expression in hypothalamus and pituitary, which suggests that TH-negative feedback has been disrupted and the HPT axis set point altered.

Several mechanisms have been proposed to explain nutritional regulation of the HPT axis, and most are centered on leptin acting directly on the TRH neuron or indirectly through neuropeptide secretion from the arcuate nucleus (18–22). In addition, prolonged nutrient deprivation has a significant effect on gene expression in the pituitary and hypothalamus (23, 24). After prolonged fasting in rodents, for example, hypothalamic *Dio2* is up-regulated (25–27), local T_3 production increases, and *Trh* repression is noted. In the anterior pituitary, in contrast, longer fasting reduces *Dio2* and *Thrb2* messenger RNA (mRNA) expression (28), and these changes tend to oppose a reduction in *Tshb* expression.

While multiple central and peripheral factors contribute to HPT repression during fasting, it remains unknown how a lower HPT set point is actually achieved and how TH-negative feedback is suppressed. Our group has previously demonstrated that THRB2 is the main mediator of TH-negative feedback in the hypothalamic TRH neuron and pituitary thyrotroph (5, 6, 29), which correlates the relatively high expression of THRB2 versus

Significance

Thyroid hormones (T_4 and T_3, TH) and fasting suppress the hypothalamic–pituitary–thyroid (HPT) axis. A mechanism for acute down-regulation of the HPT axis is described, involving phosphorylation of a thyroid hormone receptor (THR) B2 isoform at serine 101. S101 is a major THRB2 phosphorylation site not found on other THR isoforms but is present in other members of the nuclear hormone receptor superfamily. S101 is phosphorylated after T_3 binding and increases HPT axis sensitivity to T_3 inhibition. S101A is also phosphorylated by a fasting responsive pathway, yielding HPT axis suppression. A physiologically relevant THR phosphorylation function is described, permitting nutritional deprivation and TH to use a common mechanism for acute suppression of the HPT axis.

Author contributions: S.M. and F.E.W. designed research; S.M., V.D.O., S.Y.K., and H.Z. performed research; S.M., V.D.O., and H.Z. analyzed data; and S.M. and F.E.W. wrote the paper.

The authors declare no competing interest.

This article is a PNAS Direct Submission.

[1]To whom correspondence may be addressed. Email: svetam@rwjms.rutgers.edu or few11@rwjms.rutgers.edu.

This article contains supporting information online at https://www.pnas.org/lookup/suppl/doi:10.1073/pnas.2107943118/-/DCSupplemental.

Published September 20, 2021.

other THRs in the central HPT axis (6, 30, 31). In contrast, the role of THRB2 in the fasting response is less clear, although PVH *Trh* suppression in *Thrb2*$^{-/-}$ mice is partially impaired during fasting (6).

THRB2 is also unique among the THR isoforms in displaying ligand-independent action on *Trh* and *Tsh* subunit genes (32, 33). THRB2's ligand-independent property was mapped to amino acids 89 to 120 in the AF-1 domain. While exploring posttranslational modification differences among the THR isoforms using a proteomics approach, we found a major phosphorylation site on THRB2 located at serine 101 in mice (S102 in human, Fig. 1*A*). We determined that S101 in the AF-1 domain of THRB2 is highly phosphorylated in both a cultured pituitary thyrotroph (TαT1.1) cell line (5) and in the mouse pituitary and identified CDK2 as a key enzyme responsible for THRB2 phosphorylation in vitro and cultured cells.

While the S101 phosphorylation site of THRB2 is unique among THRs, several other nuclear receptors contain phosphorylation sites in the N-terminal AF-1 domain. For instance, similar sites (Fig. 1*A*) in retinoid acid receptor alpha and gamma (RARA and RARG), progesterone receptor beta, peroxisome proliferator-activated receptor gamma (PPARG), and estrogen receptor alpha (ESR1) have been shown to be phosphorylated by CDKs (34–39). Phosphorylation of these sites modulates functions of nuclear receptors in a ligand-dependent and ligand-independent manner, allowing an additional layer of regulation beyond ligand binding.

We found that phosphorylation of THRB S101 also integrated both TH and nonhormonal cues. Using *Thrb2*^{S101A} mutant mice

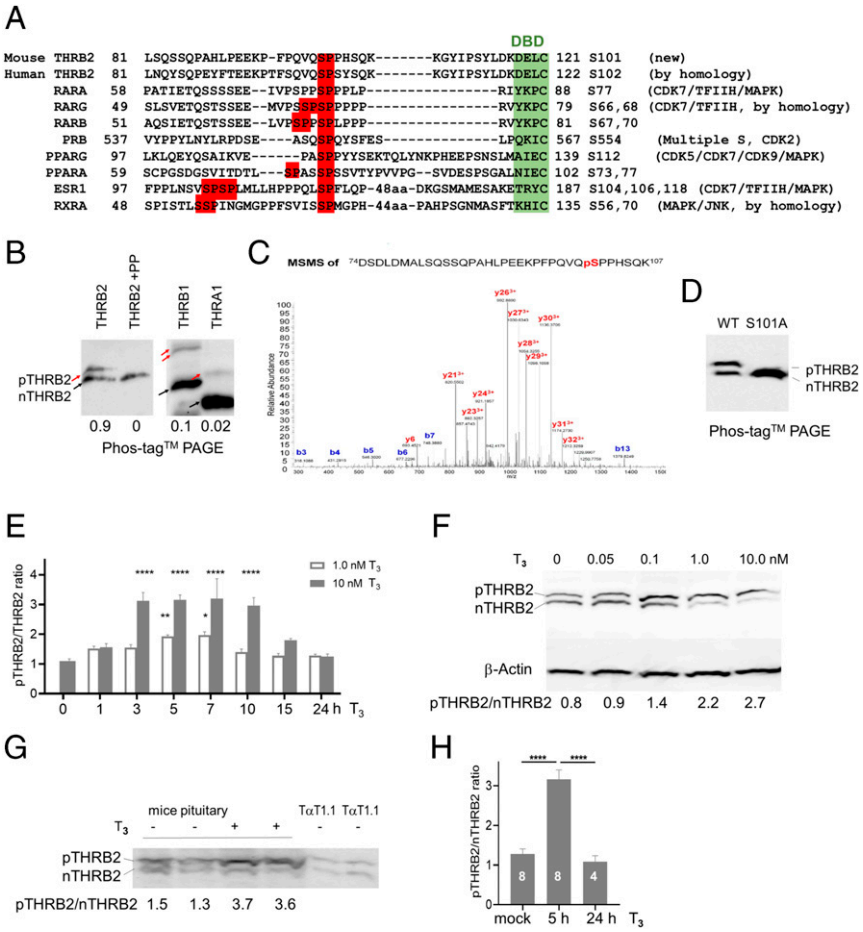

Fig. 1. Serine 101 is a major phosphorylation site in THRB2. (*A*) AF-1 domains in several nuclear hormone receptors carry a conserved site for proline-directed kinases (serine or threonine followed by proline, S/TP, red), N-terminal to the DNA-binding domain (green). The position of the site and respective kinases are shown on *Right*. (*B*) Phos-tag PAGE separation of HA-THRs expressed in TαT1.1 cells followed by Western blotting with an anti-HA antibody. THRB2 showed two major bands (phosphorylated to nonphosphorylated band intensity ratio > 0.9). The phosphorylated band disappeared upon protein phosphatase (PP) treatment (THRB2 + PP). Bands representing potential phosphorylation of THRB1 and THRA1 (high exposure used for detection, red arrows) showed about 0.1 and 0.02 intensity, respectively, compared to nonphosphorylated isoforms (black arrows). (*C*) MS/MS spectrum of the 74DSDLDMALSQSSQPAHLPEEKPFPQVQpSPPHSQK107 peptide with y (C-terminal) ion and b (N-terminal) ion peaks (phosphorylated *m/z* 3+). (*D*) Phos-tag PAGE separation of HA-THRB2 and HA-THRB2^{S101A} mutant proteins expressed in TαT1.1 cells, showing that THRB2 carries a major phosphorylation site at position 101. (*E*) T_3 treatment (1.0 and 10 nM) caused a significant increase of phosphorylated to nonphosphorylated protein intensity ratio (pTHRB2/nTHRB2) between 3 to 10 h after treatment. pTHRB2/nTHRB2 ratio from several experiments presented as a bar graph ($n > 3$). (*F*) Representative Western blot of HA-THRB2^{WT} protein expressed in TαT1.1 cells and separated in Phos-tag PAGE. Increasing T_3 concentrations (5-h treatment) caused increased THRB2 phosphorylation. Regular PAGE (4 to 20%) was used to for β-Actin Western blotting. pTHRB2/nTHRB2 ratio shown on the bottom of the blot. (*G*) Protein extracts from *Thrb2*$^{HA/HA}$ mice pituitary (30) separated by Phos-tag PAGE showed two bands matching the migration position of pTHRB2 and nTHRB2 of HA-THRB2 expressed in TαT1.1 cells. The pTHRB2/nTHRB2 ratio in mouse pituitary was increased after T_3 injection (5 h). The pTHRB2/nTHRB2 ratio is shown on the bottom of the blot. (*H*) Data from several experiments, 5 and 24 h after treatment, summarized in the bar graph, numbers of animals shown on the bars. ANOVA used for statistical analysis, values are mean ± SEM, ****$P < 0.0001$, **$P < 0.01$, *$P < 0.05$.

and TαT1.1 cells, we established that THRB2 S101 phosphorylation was essential for acute suppression of the HPT axis during fasting. We demonstrated that both TH and a key cellular energy sensor, AMP-activated kinase (AMPK), phosphorylated THRB S101 and repressed *Tshb* expression in physiologically relevant TαT1.1 cells. We propose a convergence of nutritional and TH signaling pathways on the THRB2 AF-1 domain at this phosphorylation site, providing a mechanism to adjust the HPT axis set point under a variety of metabolic states.

Results

Identification of a Novel Phosphorylation Site in THRB2. Although not extensively studied, THRs, like many other nuclear hormone receptors, are phosphoproteins (40–45), but phosphorylation is rarely detected on a Western blot, given that THR isoforms migrate on sodium dodecyl sulfate–polyacrylamide gel electrophoresis (SDS-PAGE) as single bands (5, 30). Therefore, we used Phos-tag acrylamide in SDS-PAGE (46) to separate phosphorylated and nonphosphorylated proteins. Phos-tag generally causes a unique band retardation for each phosphorylated site and/or combination of sites. HA-tagged THRs were expressed in TαT1.1 cells (5). After Phos-tag separation, we found that HA-THRB2 migrated as two major bands (Fig. 1*B*). The upper band (red arrow) was eliminated after the phosphatase treatment, indicating the upper band was pTHRB2 (Fig. 1*D*). Phos-tag separation of THRB1 and THRA1 also demonstrated retarded bands (red arrows, Fig. 1*B*), but <10% of THRB1 and <2% of THRA1 proteins were estimated to be phosphorylated.

To identify phosphorylation sites and other posttranslational modifications in THRB2 that might alter function, we expressed HA-tagged THRB2 in TαT1.1 cells both in the presence and in absence of T_3. Two combined samples of THRB2 protein were then purified using anti-HA magnetic beads and analyzed by in-gel tryptic digestion and nanoscale liquid chromatography coupled to tandem mass spectrometry (nano LC-MS/MS). The LC-MS/MS data yielded sequence coverage of ∼80% for THRB2 (*SI Appendix*, Fig. S1*A*). From both data sets, one monophosphorylated peptide was identified (Fig. 1*C*), and MS/MS spectra determined that serine 101 was phosphorylated (Fig. 1*C*). Quantitative analysis of phosphorylated and nonphosphorylated (D74-K107) peptides showed over 75% of THRB2 was phosphorylated under these conditions (*SI Appendix*, Fig. S1*B*).

To prove that the upper band represented S101 phosphorylation, we expressed a HA-THRB2 S101A (serine to alanine) mutant in TαT1.1 cells. As expected, the HA-THRB2 S101A mutant protein migrated as a single band on a Phos-tag gel and at the same position as the nonphosphorylated form of wild-type (WT) HA-THRB2 (Fig. 1*D*, nTHRB2). Thus, S101 phosphorylation of THRB2 is abundant in TαT1.1 cells and can be unambiguously detected using Phos-tag SDS-PAGE.

T_3-Dependent Regulation of THRB2 Phosphorylation. To test if the level of THRB2 phosphorylation changes in presence of its ligand (T_3), we expressed HA-THRB2 in TαT1.1 cells and treated these cells with different concentrations of T_3 for time points from 1 to 24 h (Fig. 1 *E* and *F*). We observed an increase in phosphorylation as early as 1 h after treatment, which was significantly increased between 3 and 10 h of T_3 treatment. After 24 h, the effect of T_3 on THRB2 S101 phosphorylation was lost (Fig. 1*E*). The extent of phosphorylation was dependent on T_3 concentration in which 10 nM T_3 treatment resulted in the highest THRB2 phosphorylation (Fig. 1*F*).

Since T_3 is known to promote degradation of THRB2 (47), we also determined if a lack of phosphorylation at S101 affected THRB2 levels in TαT1.1 cells. While a reduction in THRB2 protein levels was observed after 24 h of T_3 treatment (*SI Appendix*, Fig. S1*C*), there was no difference between WT and S101A mutant protein levels, suggesting that THRB2 degradation and phosphorylation were mediated by different mechanisms. T_3 is also known to affect the binding of THRB2 to corepressors and coactivators (45, 48, 49). In coimmunoprecipitation (co-IP) experiments (*SI Appendix*, Fig. S1*D*), both WT and S101A mutant proteins demonstrated similar binding to SMRT (silencing mediator of retinoid and TH receptor) and SRC-1 (steroid receptor coactivator 1). Upon T_3 treatment, the binding of SMRT to both WT and mutant THRB2 was reduced, and interaction with SRC-1 was increased, suggesting that THRB2 S101 phosphorylation does not affect interaction with these major coregulators.

To determine the role of THRB2 phosphorylation in vivo, we used $Thrb2^{HA/HA}$ mice that express endogenous HA-THRB2 (*SI Appendix*, Fig. S2 *A* and *C* (30). HA-THRB2 from pituitary extracts runs as a single band of ∼57 kDa on standard SDS-PAGE (30) but as two bands on Phos-tag SDS-PAGE, reproducing the same phosphorylation pattern as HA-$THRB2^{WT}$–expressed TαT1.1 cells (Fig. 1*G*). Average basal phosphorylation levels of THRB2 in the pituitary of euthyroid, free-fed mice are slightly higher than in TαT1.1 cells cultured without TH (pTHRB2/nTHRB2 ∼1.3 versus 1.0) and similar to phosphorylation levels of THRB2 after 0.1 nM T_3 treatment in TαT1.1 cells (Fig. 1 *E*–*H*). We compared HA-THRB2 proteins from the pituitary of T_3-treated (2 μg/100 g of body weight, intraperitoneally (i.p.) and saline-injected mice using Phos-tag SDS-PAGE and Western blotting with an anti-HA antibody. After 5 h of T_3 treatment, we detected a significant increase in phosphorylation (approximately threefold, Fig. 1 *G* and *H*), but after 24 h, the proportion of phosphorylated THRB2 returned to control levels (Fig. 1*H*). Therefore, in both cultured thyrotroph cells and mouse pituitaries, THRB2 demonstrated high monophosphorylation (∼50%), which undergoes a strong transient increase in response to TH treatment.

CDK2 Phosphorylation of THRB2 S101. THRB2 S101 is located within the N-terminal AF-1 domain, in close proximity to the DNA-binding domain and is similar in location and amino acid consensus to previously identified serine/threonine Proline (S/TP) phosphorylation sites in other nuclear hormone receptors (Fig. 1*A*). The kinases reported to phosphorylate these sites include numbers of CDKs, MAPK, and JNK (34–39, 50–52). We used NetPhos3.1 (53) to identify predicted kinases for THRB2 S101 with scores above 0.5 (CDKs, GSK3, MAPK, and RSK) for further screening using kinase inhibitors. In addition, we tested IKK, AMPK, PI3K inhibitors (*SI Appendix*, Table S1). We found that the pan-CDK inhibitor flavopiridol caused a significant reduction in THRB2 phosphorylation both in the absence and presence of T_3 (*SI Appendix*, Fig. S3*A* and Table S1). We next focused on CDK inhibitors and found that NU6027, an inhibitor of CDK1, CDK2, ATR and DNA-PK, dramatically reduced THRB2 phosphorylation at 100 μM and significantly reduced phosphorylation at 10 μM. At 100 μM, NU6027 increases HA-THRB2 expression levels in TαT1.1 cells, likely by the mechanisms unrelated to THRB2 phosphorylation (*SI Appendix*, Fig. S3*A*).

To avoid nonspecific effects of the kinase inhibitor on THRB2 expression levels and to establish a cell-free system to perform a knock-down (KD) screen, we used in vitro–translated HA-THRB2 protein and protein extract from NIH 3T3 cells. In vitro–translated HA-THRB2 ran as a single nonphosphorylated band on Phos-tag SDS-PAGE (*SI Appendix*, Fig. S3 *B* and *C*). The treatment of the in vitro–translated protein with cell extracts from NIH 3T3 in presence of ATP resulted in 25 to 45% phosphorylation of THRB2 (pTHRB2/nTHRB2 ratio of 0.4 to 0.9, *SI Appendix*, Fig. S3 *B* and *C*). Phosphorylation was inhibited by increasing concentrations of flavopiridol and NU6027 (*SI Appendix*, Fig. S3*B*). Using small interfering RNAs (siRNAs), we performed CDK KDs in NIH 3T3 cells and used protein extracts from these cells to phosphorylate in vitro–translated HA-THRB2. CDK2 was identified as the most likely candidate for THRB2 phosphorylation (*SI Appendix*, Fig. S3*C*).

To demonstrate a direct action of CDK2 on THRB2, we performed an in vitro phosphorylation assay using a purified CDK2/CycA complex. When synthesized in a coupled in vitro transcription/translation system in rabbit reticulocyte extract, both WT and S101A proteins were nonphosphorylated (Fig. 2*A*). Nearly 100% of in vitro–translated HA-THRB2^{WT} was phosphorylated within 30 min after the addition of CDK2/CycA/ATP, while the HA-THRB2^{S101A} mutant showed no related phosphorylation shift on Phos-tag gel, confirming that CDK2 specifically and directly phosphorylated S101 (Fig. 2*A*).

In human, the putative phosphorylation S/TP site (S102) is surrounded by slightly different amino acids (Fig. 1*A*). Similar to mouse proteins, we synthesized human WT and S102A proteins in a coupled in vitro transcription/translation system and treated it with CDK2/CycA/ATP (*SI Appendix*, Fig. S4*A*). WT protein showed about 60% phosphorylation, while the HA-THRB2^{S102A} mutant showed no related phosphorylation shift on Phos-tag gel, confirming that CDK2 was able to phosphorylate S102 in human THRB2. Furthermore, we expressed both proteins in HEK293 cells. WT protein showed ~30% phosphorylation (pTHRB2/nTHRB2 ~0.4), which was significantly reduced by CDK inhibitor flavopiridol (pTHRB2/nTHRB2 ~0.2, *SI Appendix*, Fig. S4 *B* and *C*). The pTHRB2 band was not detected in the THRB2S102^{A} protein (*SI Appendix*, Fig. S4*B*), proving that human THRB2 is highly phosphorylated at the equivalent serine residue and targeted by CDKs.

CDK2/CycA-Mediated Phosphorylation of S101 Affects THRB2 DNA Binding. THRs interact with DNA (DR4 elements) as both a homodimer or a heterodimer with Retinoid X Receptor (RXR) (54–56). Using an electromobility gel-shift assay (EMSA), we tested the binding characteristics of WT and S101A THRB2 proteins in the absence and in presence of CDK2/CycA-dependent phosphorylation. Nonphosphorylated WT and S101A THRB2 proteins were able to form homodimers on the DR4 element, which were dissociated in a T_3 concentration-dependent manner as previously reported (Fig. 2*B*) (5). The addition of CDK2/CycA induced phosphorylation of WT THRB2 (Fig. 2*A*) and significantly reduced homodimerization on the DR4 element (Fig. 2 *B* and *C*). In contrast, CDK2/CycA treatment did not affect THRB2^{S101A} homodimer binding to DR4.

An EMSA of the DR4 element in the presence of RXRA and THRB2 showed strong heterodimer binding (Fig. 2 *D* and *E*), which was further increased after CDK2/CycA/ATP treatment. No change in heterodimer binding was observed for the S101A mutant protein. Thus, S101 phosphorylation of THRB2 reduced homodimeric and enhanced heterodimeric binding with RXRA on a DR4 element, indicating that the S101 phosphorylation regulated THRB2 DNA binding by a T_3-independent mechanism.

Effect of S101 Phosphorylation on T_3 Regulation of the HPT Axis. To test if the mutation of S101 affected TH-dependent gene expression in vitro, we knocked down endogenous *Thrb* in a thyrotroph cell line (TαT1.1) and re-expressed HA-THRB2^{WT} and HA-THRB2^{S101A} at equal levels using a previously established method (Fig. 2*F*) (5). T_3-dependent expression of target genes (*Tshb*, *Rab27b*, and *Sema3c*) were measured using qRT-PCR (Fig. 2 *G* and *H*).

HA-THRB2^{WT} gradually repressed *Tshb* expression at T_3 concentrations ranging from 0.1 to 10 nM and showed significant reduction of *Tshb* mRNA at 0.2 nM. HA-THRB2^{S101A} was less effective in reducing *Tshb* expression at low T_3 concentrations (Fig. 2 *G* and *H*) but equally effective at reducing *Tshb* expression at concentrations of 0.5 nM and higher (Fig. 2 *G* and *H*). In contrast, HA-THRB2^{WT} and HA-THRB2^{S101A} functioned similarly in T_3-dependent positive regulation on at least two genes (Fig. 2*H*). These results suggest that the S101A mutation selectively affected gene expression of *Tshb* at low to euthyroid levels of TH.

In order to assess the effect of THRB2 phosphorylation in control of the HPT axis in vivo, we generated *Thrb2*^{S101A} knock-in mice (*SI Appendix*, Fig. S2*A*, asterisk). These mice developed normally, and litter sizes and body weights of *Thrb2*$^{S101A/S101A}$ mice on a regular chow diet were similar to that of WT. The mutation did not affect expression levels of *Thrb2*, *Thrb1*, or *Thra1* in either the pituitary or hypothalamus (*SI Appendix*, Fig. S2*B*). Similar to data from TαT1.1 cells (*SI Appendix*, Fig. S1*C*), the S101A mutation did not affect protein level or stability of THRB2 in the mouse pituitary (*SI Appendix*, Fig. S2 *C* and *D*).

Serum free T_4 (fT_4), free T_3 (fT_3), and TSH levels in *Thrb2*$^{S101A/S101A}$ mice were not significantly different from that in WT controls in free-fed (FF) conditions (Fig. 3 *A*–*C*). We next placed mice on a low iodine/propylthiouracil (LoI/PTU) diet to achieve hypothyroidism followed by a TSH suppression test using increasing concentrations of T_3. During the hypothyroid phase, the TSH response was similar between WT and *Thrb2*$^{S101A/S101A}$ (*SI Appendix*, Fig. S2*E*). However, the *Thrb2*$^{S101A/S101A}$ response during T_3 suppression appeared to be less robust, although lacking a statistically significant difference, at the 0.5 μg/100 g body weight (BW) dose, which is a dose that, in combination with a LoI/PTU diet, mimics the euthyroid condition in mice (*SI Appendix*, Fig. S2*F*).

The S101A Mutation in Mice *Thrb2* Reduced Responsiveness of HPT Axis to Fasting. We next tested the response of the HPT axis to short- and long-term fasting. We compared serum fT_4, fT_3, and TSH levels (Fig. 3 *A*–*C*) in *Thrb2*^{WT} and *Thrb2*$^{S101A/S101A}$ FF and fasted animals. In WT animals, TSH decreased significantly after 12 and 24 h of fasting (Fig. 3*C*), and the levels of fT_4 and fT_3 declined, respectively (Fig. 3 *A* and *B*). In contrast, *Thrb2*$^{S101A/S101A}$ mice showed no change in fasting serum fT_3 levels and a blunted response in TSH levels, although fT_4 levels were reduced similar to that in WT (Fig. 3 *A*–*C*). While serum fT_3 levels appear to depend on the central HPT axis, changes in circulating fT_4 are consistent with a peripheral increase in DIO3 expression and activity (17, 57).

To determine if differences in serum TSH between WT and *Thrb2*$^{S101A/S101A}$ mice resulted from differences in *Tshb* expression, we compared *Tshb* mRNA levels in pituitaries of FF and fasted mice. In WT animals, *Tshb* mRNA levels were significantly reduced after 12 h of fasting and were further decreased after 24 h to about 50% of FF levels. In *Thrb2*$^{S101A/S101A}$ mice, no difference in *Tshb* expression was observed in 12-h fasted mice compared to FF mice, although 24-h fasted mice had a ~30% reduction of *Tshb* mRNA (Fig. 3*D*).

Given the localization of THRB2 in both anterior pituitary thyrotrophs and the paraventricular nucleus of the hypothalamus (PVN), we next examined PVN TRH levels in WT and *Thrb2*$^{S101A/S101A}$ FF and 24-h fasted mice. As previously reported, fasting reduced TRH mRNA levels in WT mice (6), and these data on TRH levels were consistent (Fig. 3 *E* and *F*). In contrast, TRH levels were unchanged in 24-h fasted *Thrb2*$^{S101A/S101A}$ mice. In summary, the central HPT axis (TRH neuron and thyrotroph) showed resistance to the effects of short-term fasting in S101A mutant mice.

Fasting and AICAR Treatment Increase THRB2 Phosphorylation in the Mouse Pituitary. THRB2 protein levels in PVN are insufficient for the Phos-tag assay, but we were able to observe a significant increase in pTHRB2/nTHRB2 in the pituitary (2.5-fold, Fig. 3 *G* and *H*) after 5 h of fasting. Interestingly, THRB2 phosphorylation returned to basal levels after 24 h of fasting (Fig. 3*H*), which was similar to the phosphorylation response after T_3 treatment (Fig. 1 *G* and *H*).

Fasting-induced suppression of the HPT axis is controlled by leptin (58) and potentially by other nutritional and hormonal signals, including ghrelin, insulin, GLP-1, glucagon, many of which function through AMPK activation (59, 60). Fasting also

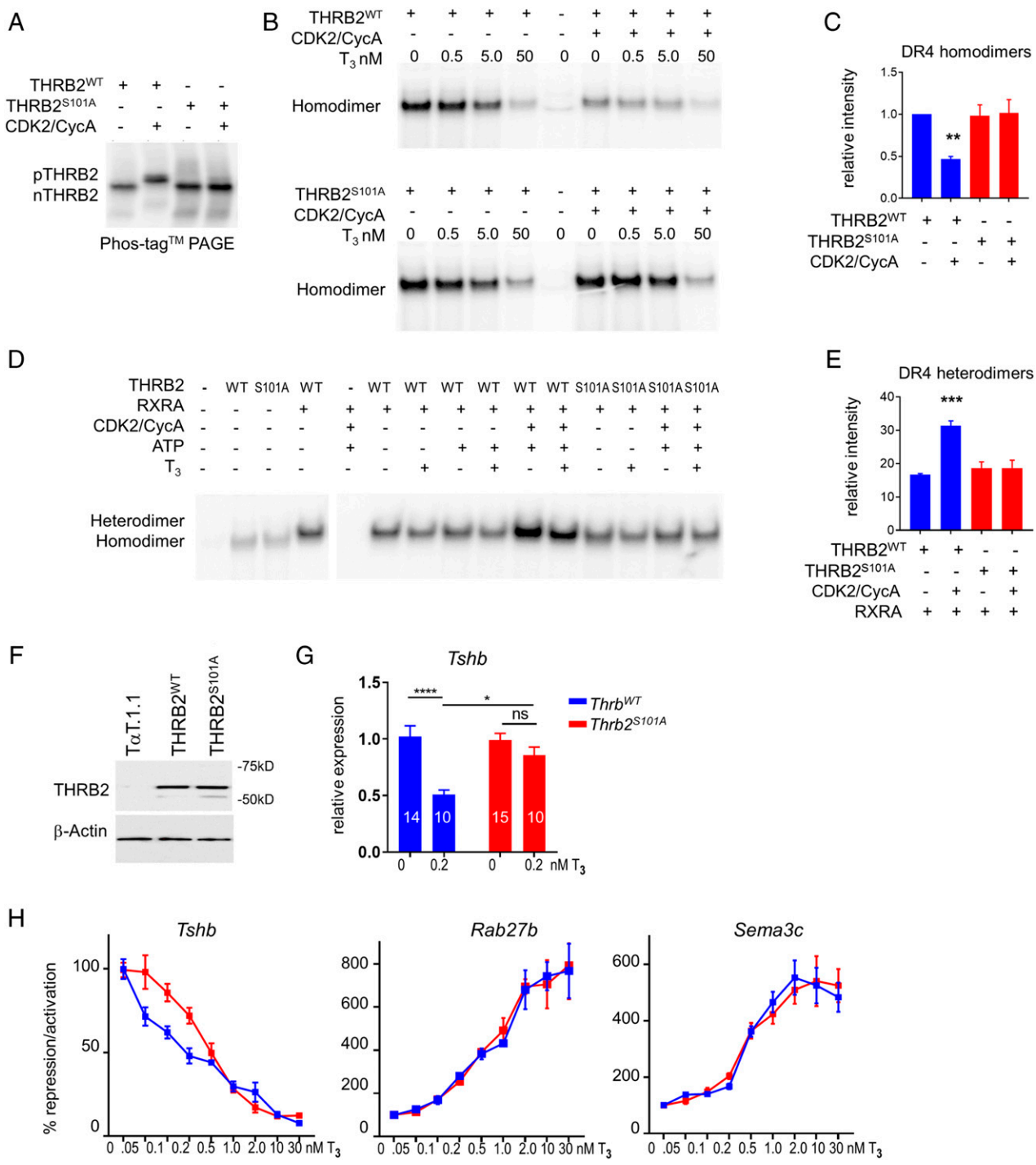

Fig. 2. CDK2/CycA-dependent phosphorylation of THRB2 S101 and its effect on DNA binding and transcription. (*A*) In vitro transcription/translation proteins from rabbit reticulocyte lysate extracts were treated with CDK2/CycA in the presence of ATP and analyzed by Phos-tag PAGE/Western blotting and an anti-HA antibody. Nearly 100% of WT protein showed a phosphorylation shift, while the migration position of THRB2^{S101A} protein was not altered. (*B*) Binding of WT and S101A mutant proteins to DR4 element was tested by EMSA. WT and mutant homodimers gradually dissociated with increasing T_3 concentrations. CDK2/CycA treatment significantly reduced homodimer formation for WT but not for mutant protein. (*C*) Bar graph summarizing data from three experiments. Band intensity was normalized to the level of untreated WT homodimer. (*D*) In presence of RXRA, both WT and S101A mutant proteins formed heterodimers on DR4 (heterodimer bands migrate higher and ~10 to 15 times stronger in intensity than homodimer) both in absence and presence of T_3 (50 nM). The addition of CDK2/CycA significantly increased binding of WT protein but did not affect S101A heterodimer DNA binding. (*E*) Bar graph with data from three experiments, band intensity normalized to WT untreated homodimer in each experiment. WT protein binding intensity shown in blue and S101A mutant protein in red. (*F*) HA-THRB2^{WT} and HA-THRB2^{S101A} proteins expressed in *Thrb2 KD* TαT1.1 cells were tested by Western blotting (4 to 20% PAGE) with anti-HA and β-Actin antibodies. (*G*) After *Thrb KD* in TαT1.1 cells, re-expression of *HA-Thrb2^{WT}* (*Thrb2^{WT}*, blue) but not *Thrb KD HA-Thrb2^{S101A}* (*Thrb2^{S101A}*, red) significantly repressed *Tshb* at 0.2 nM of T_3. The numbers of replicates shown on the bar graph. (*H*) Gene repression (*Tshb*) and activation (*Rab27b, Sema3c*) were tested in TαT1.1 cells across a wide range of T_3 concentrations. Data collected from three experiments, normalized to expression levels (100%) at 0 nM T_3, and presented as % activation/repression, $n > 3$ in each experiment. Relative expression of T_3-regulated genes were measured by qRT-PCR and normalized to *Actb* and *Rpl13a* mRNAs. Values are mean ± SEM, ****$P < 0.0001$, ***$P < 0.001$, **$P < 0.01$, *$P < 0.05$, ns for not significant.

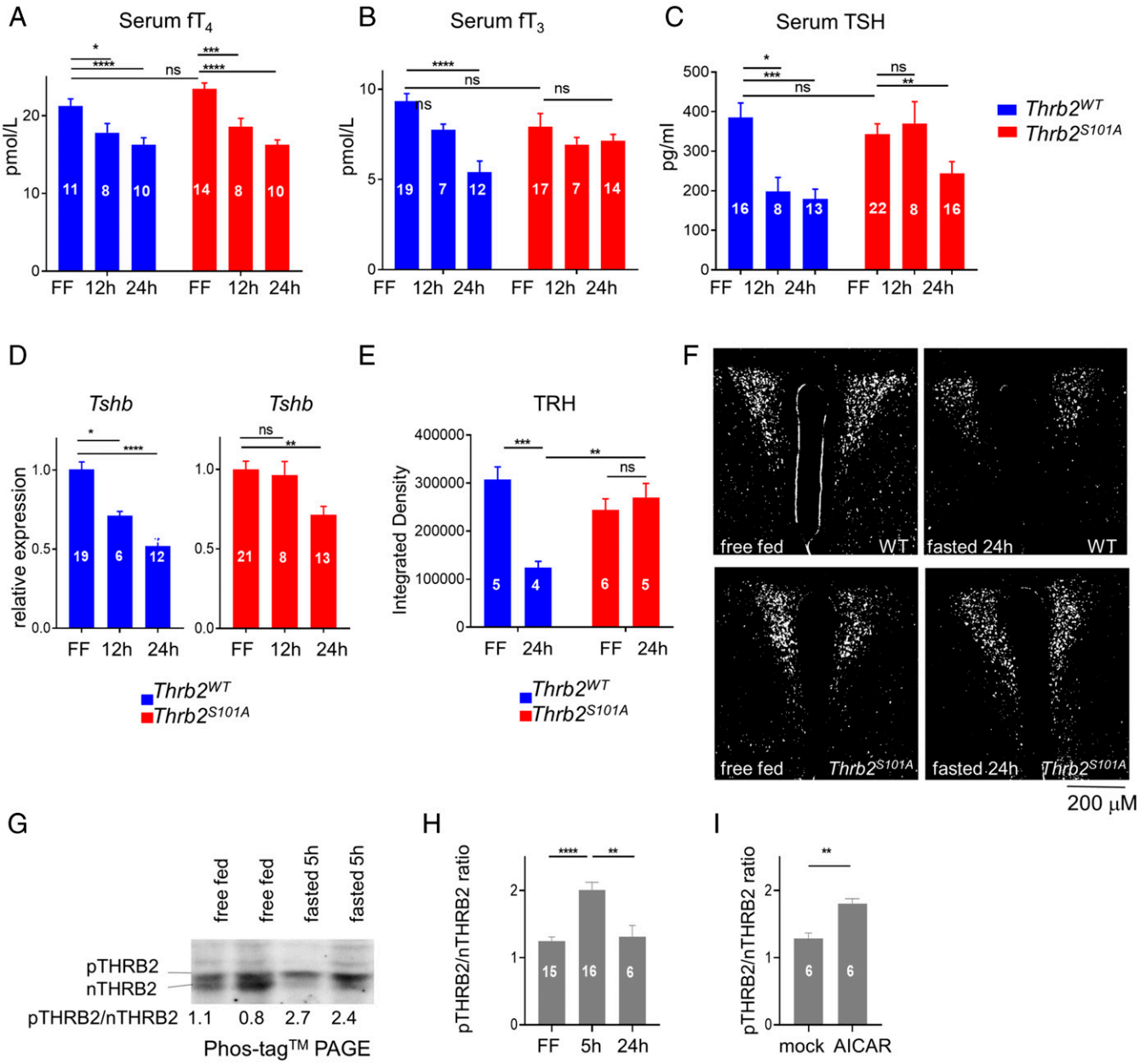

Fig. 3. Effect of THRB2 S101 phosphorylation on TH levels and HPT set point during fasting. (*A*–*C*) Serum hormones were measured in FF and 12-h and 24-h fasted state. (*D*) *Tshb* relative expression in mouse pituitary was measured by qRT-PCR and normalized to *Rpl13a*. In WT animals (blue), fasting caused a reduction of serum fT_4 (*A*), serum fT_3 (*B*), serum TSH (*C*), and pituitary *Tshb* mRNA levels (*D*). $Thrb2^{S101A/S101A}$ animals (red) in contrast showed no significant down-regulation of serum fT_3, TSH, and *Tshb* after 12 h of fasting. After 24 h of fasting, serum fT_3 was unchanged and TSH and *Tshb* were suppressed but less than WT mice. (*E*) Bar graph summarizing measurements of integrated density of TRH in individual animals. In WT (blue), PVH TRH decreased after fasting, but no change was observed in mutant PVNs (red). (*F*) Representative anti-TRH staining (immunofluorescence) showing the response of TRH in the rostral PVN to 24 h fasting in WT and $Thrb^{S101A/S101A}$ animals. (Scale bar, 200 µm.) (*G*) Western blot (Phos-tag PAGE, anti-HA antibody) showing an increase in HA-THRB2 phosphorylation ($Thrb2^{HA/HA}$ mice, pituitary) after 5 h of fasting. Phosphorylated to nonphosphorylated protein intensity ratio (pTHRB2/nTHRB2) shown on the bottom of the blot. (*H*) Bar graph summarizing data from FF and 5-h and 24-h fasted animals. (*I*) Bar graph showing increase in THRB2 phosphorylation in response to AICAR injection (i.p., 400 mg/kg BW, 5 h). The numbers of mice are shown on the bar graphs, and values are mean ± SEM, $^{****}P < 0.0001$, $^{***}P < 0.001$, $^{**}P < 0.01$, $^{*}P < 0.05$, ns for not significant.

reduces cellular energy and increase the AMP-ADP/ATP ratio, leading to AMPK activation (61). Although the extracellular mediator of the acute fasting response of the HPT central axis is presently unknown, we tested if i.p. injection of the AMP analog, 5-aminoimidazole-4-carboxamide ribonucleotide (AICAR), could induce THRB2 phosphorylation. Interestingly, a single injection of AICAR caused a moderate but statistically significant increase in THRB2 phosphorylation in vivo (Fig. 3*I*).

Role of AMPK in THRB2 Phosphorylation and Control of the HPT Axis. The fasting and activation of AMPK affect metabolism through action on the central axis (hypothalamus and anterior pituitary), thyroid, autonomic nervous system, and peripheral tissues. To test the direct and cell autonomous effect of reduced cellular energy and AMPK activation on THRB2 phosphorylation, we employed the TαT1.1 cell line since it is the only available in vitro physiologically relevant model of the HPT axis.

The TαT1.1 cell model separates the effects of T_3 and AMPK activation on the thyrotroph from hypothalamic TRH stimulation and peripheral signals. We tested AMPK activators, AICAR and PF-06409577, on phosphorylation of HA-THRB2 in TαT1.1 cells. Both activators triggered a short-term increase in HA-THRB2 phosphorylation (~1 h, *SI Appendix*, Fig. S5), but selective allosteric activator PF-06409577 caused the most stable AMPK activation and THRB2 phosphorylation and was used for further experiments (Fig. 4).

To assure specificity of PF-06409577 for AMPK activation, we also used an AMPK competitive inhibitor, Dorsomorphin/Compound C (Fig. 4 *A*–*D*). Compound C suppressed both AMPK activation (Fig. 4*B*) and additional phosphorylation of HA-THRB2 mediated by PF06409577 and T_3 (Fig. 4 *C* and *D*). Because AMPK is not the kinase that directly phosphorylates THRB2, we tested if AMPK-mediated THRB2 phosphorylation would be blocked by a CDK inhibitor. Indeed, the CDK1/2 inhibitor NU6027 blocked PF-06409577/AMPK-induced phosphorylation (Fig. 4*E*).

Furthermore, we found that PF-06409577 treatment of TαT1.1 cells caused a reduction in Tshb expression (Fig. 4*G*). This effect was completely lost in Thrb KD cells (Fig. 4 *H* and *I*), confirming that Thrb was required for both T_3- and AMPK-dependent repression of Tshb. To test the role of THRB2 phosphorylation on Tshb repression, we re-expressed HA-$THRB2^{WT}$ and HA-$THRB2^{S101A}$ at equal levels in TαT1.1 cells (Fig. 4*J*). AMPK-dependent Tshb repression was restored by re-expression of HA-$THRB2^{WT}$ but not by HA-$THRB2^{S101A}$ (Fig. 4 *K* and *L*). Consistent with previous data (Fig. 2), HA-$THRB2^{S101A}$ was unable to repress Tshb at 0.2 nM T_3 but exhibited normal repression at 2.0 nM (Fig. 4*L*). Unlike T_3 (*SI Appendix*, Fig. S1*C*), PF-06409577 treatment did not cause THRB2 degradation or any significant change in protein abundance (Fig. 4*J*). Taken together, our data demonstrate that S101 phosphorylation is increased by either AMPK or T_3 treatment. The increase of THRB2 phosphorylation resulted in repression of Tshb in either case, indicating a ligand-independent effect of THRB2 phosphorylation on gene expression.

Discussion

Effects of Fasting and Role of AMPK Activation on THRB2 Phosphorylation and HPT. The HPT axis is exquisitely sensitive to TH-negative feedback, allowing serum TSH-dependent regulation of TH levels near a set point established for each individual (Fig. 4*M*) (1, 2). In particular, T_3 bound to THRB2 is known to suppress both *Trh* and *Tsh* subunit gene expression (5, 6, 31). Like TH, nutrient deficiency also down-regulates the HPT axis (8, 10–12); however, little is known about mechanisms establishing the HPT set point and whether the HPT negative feedback mechanisms of TH and fasting are related.

The relationship between nutrient and TH regulation of the HPT axis has been investigated by several laboratories. After the discovery of leptin, Ahima et al. showed that fasting-induced suppression of the HPT axis was mediated in part by a reduction in leptin secretion (58). Subsequently, other pathways were implicated in the fasting response of the HPT axis (reviewed in refs. 1 and 62). For example, leptin feedback was defined as both activating the PVN TRH neuron directly and indirectly via neuropeptides from the arcuate nucleus (16, 19).

In this study, we provide a plausible mechanism implicating THRB2 N-terminal phosphorylation in set-point regulation by both TH and nutritional status. Using *Thrb2*$^{S101A/S101A}$ mice, we show that phosphorylation of THRB2 is required for robust down-regulation of TRH and TSH during fasting (Fig. 3). The HPT axis, however, is regulated at multiple levels (hypothalamus, anterior pituitary, and thyroid), which complicates the study of the HPT set point in vivo. We therefore used a permanent thyrotroph cell line (TαT1.1 cells) that expresses endogenous TSH and is regulated by T_3 (5). In cultured thyrotrophs and pituitary, we found little or no leptin effect on THRB2 phosphorylation and *Tshb* expression, likely because of low levels of LepRb expression in these cells. Instead, we discovered that a universal energy sensor, AMPK, activated THRB2 phosphorylation and mediated *Tshb* repression (Figs. 3 and 4). PF-06409577–mediated AMPK activation, for example, caused a reduction in *Tshb* mRNA levels in TαT1.1 cells independent of TH. This effect required THRB2 and an intact serine at position 101. The S101A mutation in THRB2 not only abolished suppression of *Tshb* mRNA levels by PF-06409577 but also blunted *Tshb* repression at low concentrations of T_3 (Fig. 2 *G* and *L*). These in vitro data are consistent with phenotypes of *Thrb2*$^{S101A/S101A}$ mice (Fig. 3), indicating that THRB2 S101 phosphorylation during fasting functions to repress *Trh* and *Tshb* subunits and increases sensitivity of the HPT axis to low concentrations of THs (Fig. 4*M*).

AMPK integrates extracellular nutritional and hormonal signals mediated by leptin, ghrelin, insulin, GLP-1, glucagon, and TH signaling pathways (59, 60, 63) but also functions as a direct intracellular sensor of energy charge (reviewed in refs. 61 and 64). The relationship between AMPK and THs has been studied in the brain, where T_3 administration appears to decrease the activity of hypothalamic AMPK (63). A direct effect of AMPK on the HPT axis has not been well studied, although its role can be inferred from data showing that metformin (a known AMPK activator) decreases serum TSH and TH levels (65–67).

Role of CDK2-Mediated Phosphorylation in THRB2 DNA Binding and Transcriptional Control of *Tshb*. THRs are known to be phosphorylated at several sites based on in vitro studies (40–45, 68). Unfortunately, none of these studies compared relative phosphorylation among the various THRs, provided in vivo evidence of a physiological effect of phosphorylation, or evaluated the THRB2 isoform. Indeed, when we compared HA-THRs expressed in TαT1.1 cells, THRA1 and THRB1 were weakly phosphorylated (<10% of total receptor protein is phosphorylated, Fig. 1*B*). In contrast, a single major phosphorylation site in THRB2 was found, which was 30 to 85% phosphorylated depending on conditions. THRB2 S101 (S102 in human) is located in the most divergent AF-1 domain of THRs and is a part of the S/TP motif, typically phosphorylated by CDKs and MAPK. This site is absent in THRB1 and THRA1/2 but found in several nuclear receptors (Fig. 1*A*), including S118 of ESR1 and S112 of PPARG (50, 69, 70).

Using a combination of kinase inhibitors and siRNA (*SI Appendix*), we identified CDK2 as the most potent kinase acting on S101. A CDK2/CycA purified complex was able to phosphorylate nearly 100% of in vitro–translated THRB2 protein, proving a direct action of this kinase on the S101 site (Fig. 2*A*). CDK inhibitors (flavopiridol/NU6027) significantly reduced but did not eliminate THRB2 S101 and S102 phosphorylation in TαT1.1 and in HE293 cells (Fig. 4*E* and *SI Appendix*, Figs. S2*A* and S4*B*), leaving open the possibility that other kinases may target the same site. Consistent with this finding, the S/TP motif is often targeted by multiple kinases. For example, PPARG S118 is phosphorylated by MAPK, CDK5, CDK7, and CDK9 (34, 35, 50, 52, 70) and ESR1 S112 by CDK7 and MAPK (69). However, in our studies, three MAPK inhibitors failed to reduce basal or T_3-mediated THRB2 phosphorylation (*SI Appendix*, Table S1).

Both AMPK and T_3 mediate S101 phosphorylation in THRB2, resulting in *Tshb* repression in thyrotrophs, and appear to have an additive effect at least in vitro (Fig. 4 *D* and *G*). We suggest that both AMPK activation and T_3 result in CDK2-dependent phosphorylation of S101 (Fig. 4 *E*, *F*, and *M* and *SI Appendix*, Fig. S3). Interestingly, T_3 has been previously reported to increase CDK2 levels (71). How AMPK activates CDK2 function remains unclear, but Short et al. suggested that AMPK signaling may result in cytoplasmic sequestration of p27, which

CELL BIOLOGY

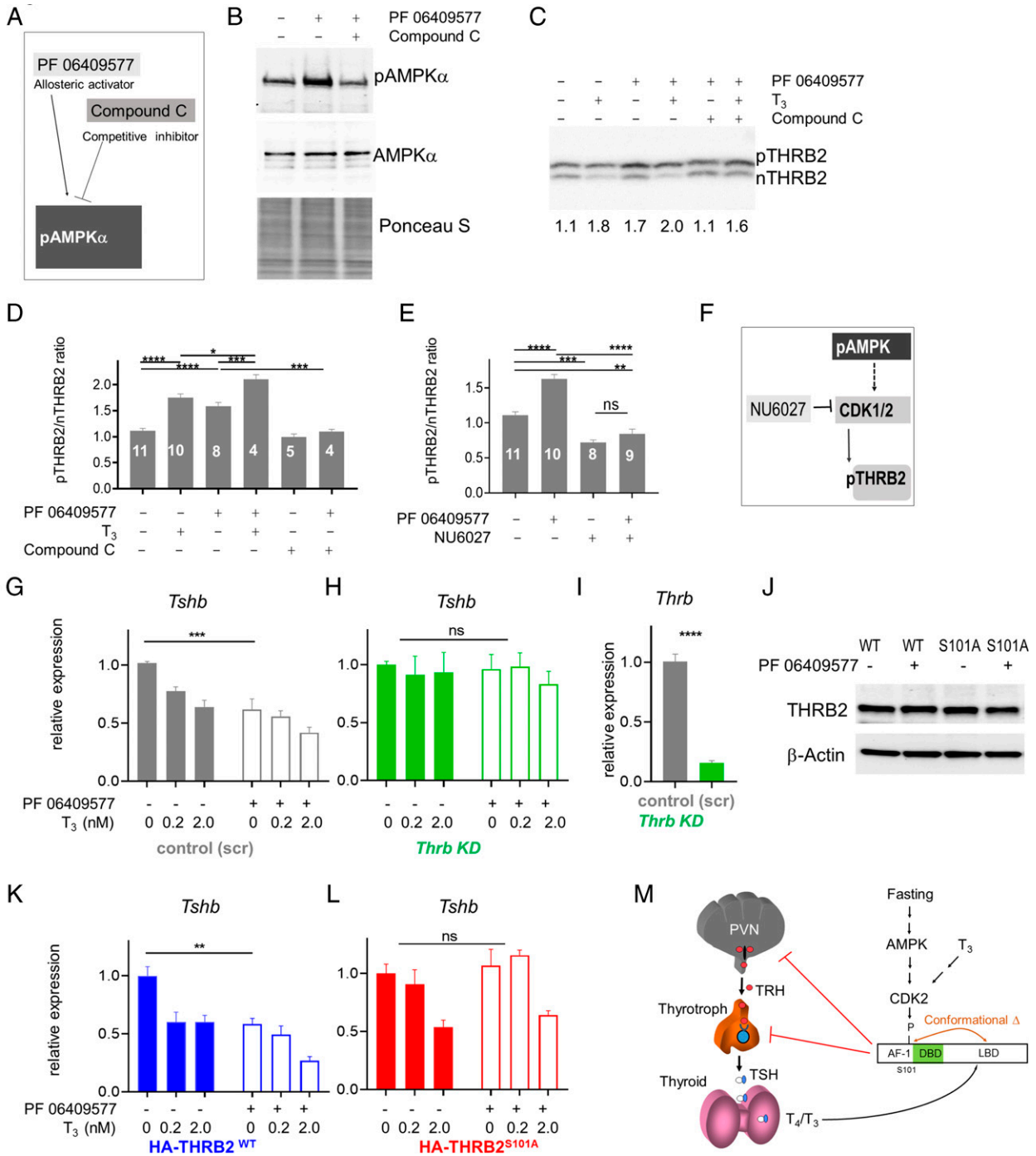

Fig. 4. Effect of AMPK on THRB2 S101 phosphorylation and *Tshb* expression in TαT1.1 cells. (*A*) Schematic representation of the action of AMPK activator (PF-06409577) and inhibitor (Compound C). (*B*) Western blot of TαT1.1 cell extracts probed with anti-pAMPK and anti-AMPK antibodies, demonstrating activation of phosphorylation of AMPK (pAMPK) by PF-06409577 and inhibition by Compound C. Ponceau S staining and total AMPK served as loading controls. (*C*) Representative Phos-tag PAGE Western blot of HA-THRB2 protein expressed in TαT1.1 cells treated with PF-06409577 (2.5 μM), T_3 (1 nM), and Compound C (5 μM). Intensity ratio of phosphorylated to nonphosphorylated protein (pTHRB2/nTHRB2) shown on the bottom of the blot. (*D*) Bar graph represents the pTHRB2/nTHRB2 ratio from several experiments with total number of replicates on each bar. (*E*) Bar graph showing reduction in phosphorylation (pTHRB2/nTHRB2 ratio) upon treatment with CDK1/2 inhibitor NU6027 (10 μM). (*F*) Schematic representation of the action of a NU6027 on a pAMPK–CDK1/2–pTHRB2 pathway. The inhibition of CDK1/2 reduced both basal and AMPK-dependent THRB2 phosphorylation. (*G*) PF-064095077 (2 μM) caused a significant reduction of *Tshb* expression independent of T_3 in TαT1.1 cells (*scr* short hairpin RNA (shRNA) control, gray). (*H*) *Thrb* KD (green) abolished both T_3- and PF-064095077/AMPK-dependent *Tshb* repression. *Tshb* (*G*, *H*, *K*, and *L*) and *Thrb* (*I*) relative expression was measured by qRT-PCR and normalized to *Rpl13a*. (*J*) HA-THRB2^{WT} and HA-THRB2^{S101A} proteins were re-expressed in *Thrb KD* TαT1.1 cells and tested by Western blotting (4 to 20% PAGE) with anti-HA antibody and β-Actin for loading control. (*K*) Re-expression of WT THRB2 (*Thrb2 KD HA-Thrb2^{WT}*) TαT1.1 cells (blue) rescued both T_3-dependent and PF-064095077/AMPK-dependent *Tshb* repression. (*L*) THRB2^{S101A} (*Thrb2 KD HA-Thrb2^{S101A}*) restored T_3-dependent *Tshb* repression at 2 nM of T_3, but it did not rescue low-dose T_3 or AMPK-dependent *Tshb* regulation. Bar graph values are mean ± SEM, $n = 4$, ****$P < 0.0001$, ***$P < 0.001$, **$P < 0.01$, *$P < 0.05$, ns for not significant. ANOVA used for statistical analysis. (*M*) Model, illustrating effect of fasting on THRB2 S101 phosphorylation, and HPT axis (AMPK/CDK2 regulation inferred from biochemical and in vitro experiments).

would then elevate CDK2 nuclear activity (72). In EMSA, CDK2-induced THRB2 S101 phosphorylation correlated with increased THRB2/RXRA heterodimer and reduced THRB2 homodimer binding to a DR4 element (Fig. 2). Our laboratory has previously associated THRB2 homodimer formation in EMSA with TH-negative regulation (5, 73). It is conceivable that S101 phosphorylation selectively affects negative regulation of transcription by altering THRB2 DNA binding.

Phosphorylation of the AF-1 S/TP site in other nuclear receptors (Fig. 1*A*) also affects DNA binding, and two major mechanisms have been proposed: conformational change by serine-proline bond isomerization (74) and the recruitment of CDKs and other coregulators to DNA (75, 76). For example, S/TP sites in PR are suggested to recruit a CDK2/CycA complex to promoters, where it facilitates phosphorylation of coactivators such as SRC-1 (75). CDK2 recruitment to promoters may also induce phosphorylation of poly-(ADP)-ribose polymerase (PARP-1), cause local displacement of H1 linker histones, and induce chromatin remodeling (76). Phosphorylation of ESR1 S118 enhances DNA binding and increases transcriptional activity through recruitment of peptidyl prolyl *cis/trans* isomerase Pin1 (74). Finally, and most similar to THRB2, phosphorylation of RARA Ser-77 by CDK7/CycH (Fig. 1*A*) increases efficiency of RARA/RXR heterodimer binding in EMSA (39). Taken together, the S/TP motifs found in the AF-1 domain of THRB2, and several other nuclear receptors, may utilize common mechanisms to alter DNA binding and change transcription. Similar to other nuclear receptors, THRB2 AF-1 phosphorylation has a selective effect on target gene expression, repressing *Tshb* and possibly *Trh* but not altering expression of genes like *Rab27b* or *Sema3c*.

By promoting S101 THRB2 phosphorylation, fasting utilizes the same pathway as T_3 to suppress the HPT axis. This establishes a new lower set point in the HPT axis, which is resistant to the effects of lower TH levels. In humans, significant changes in HPT axis set point and circulating TH concentrations are also found in the nonthyroidal illness syndrome, which is due to a broad range of disorders such as trauma and surgery. Given that suppression of the HPT axis appears to happen sooner in rodents than humans, extrapolation to the human disease may be difficult. Nonetheless, human THRB2 carries the same site (S102, Fig.1*A*) targeted by CDKs in vitro (*SI Appendix*, Fig. S4); and importantly, AMPK activation by metformin reduces serum TSH and TH levels in men (62–64). Therefore, S101/102 phosphorylation may represent the convergence of nutritional and TH signaling pathways at THRB2 in both mice and humans and a pathway to regulate the HPT axis.

Materials and Methods

Functional assays in TαT1.1 cells, *Thrb KD*, and HA-THRB2 rescue experiments were performed as previously described (5). For phosphorylation analysis, proteins were separated using 9% SDS-PAGE containing 100 μM MnCl and 50 μM Phos-tag acrylamide (Phos-tag, AAL-107, Wako Chemicals). Full details for cell culture experiments, qRT-PCR, oligonucleotides, antibody information, in vitro assays, cell-free assays, and mass spectrometry are available in *SI Appendix, Supplemental Materials and Methods*.

All animal experiments were approved by the Institutional Animal Care and Use Committee of Rutgers, The State University of New Jersey. All mice had a C57BL/6J genetic background and were maintained on a standard diet (no. 5008, LabDiet) with water ad libitum in a temperature-controlled facility with a 12-h light/12-h dark schedule. Unless otherwise indicated, 3- to 3.5-mo-old adult males were used for serum and tissue collection. *Thrb2*^{HA} mice were previously characterized, and the difference between levels of THRB2 expression and TSH levels in male and female were noted (30). Therefore, only males were used in this study. *Thrb2*^{S101A} mutant mice were generated by Genome Editing Shared Resource, Rutgers University, using the CRISPR-Cas9 technique. The detailed technique, as well as hormone measurements, tissue collection, and immunofluorescence are available in *SI Appendix, Supplemental Materials and Methods*.

Data Availability. All study data are included in the article and/or *SI Appendix*.

ACKNOWLEDGMENTS. We thank Dr. Arnold Rabson, Dr. Peter Romanenko, Dr. Ghassan Yehia, and Dr. Peter Lobel for discussion and help at the initiation of the project and Dr. Xiaoyang Su, Michael Brotherton, Sanya Bansal, and Katarzyna Kalemba for technical help and advice, as well as all members of the laboratory and department of Medicine, Robert Wood Johnson Medical School for scientific discussions. The funding was from NIH DK R0149126 (F.E.W.) and P30 CA072720 (Cancer Institute of New Jersey) and mass spectrometry equipment Grant NIH S10OD016400. Mouse models were generated by Rutgers Cancer Institute of New Jersey Genome Editing Shared Resource P30CA072720-5922. Robert Wood Johnson Foundation Grant No. 74260 supports the Child Health Institute of New Jersey and the use of shared resources.

1. A. C. Bianco *et al*., Paradigms of dynamic control of thyroid hormone signaling. *Endocr. Rev.* **40**, 1000–1047 (2019).
2. T. M. Ortiga-Carvalho, A. R. Sidhaye, F. E. Wondisford, Thyroid hormone receptors and resistance to thyroid hormone disorders. *Nat. Rev. Endocrinol.* **10**, 582–591 (2014).
3. F. Chatonnet, R. Guyot, G. Benoît, F. Flamant, Genome-wide analysis of thyroid hormone receptors shared and specific functions in neural cells. *Proc. Natl. Acad. Sci. U.S.A.* **110**, E766–E775 (2013).
4. P. Ramadoss *et al*., Novel mechanism of positive versus negative regulation by thyroid hormone receptor β1 (TRβ1) identified by genome-wide profiling of binding sites in mouse liver. *J. Biol. Chem.* **289**, 1313–1328 (2014).
5. V. M. S. Pinto *et al*., Naturally occurring amino acids in helix 10 of the thyroid hormone receptor mediate isoform-specific TH gene regulation. *Endocrinology* **158**, 3067–3078 (2017).
6. E. D. Abel, R. S. Ahima, M. E. Boers, J. K. Elmquist, F. E. Wondisford, Critical role for thyroid hormone receptor beta2 in the regulation of paraventricular thyrotropin-releasing hormone neurons. *J. Clin. Invest.* **107**, 1017–1023 (2001).
7. E. D. Abel *et al*., Dominant inhibition of thyroid hormone action selectively in the pituitary of thyroid hormone receptor-beta null mice abolishes the regulation of thyrotropin by thyroid hormone. *Mol. Endocrinol.* **17**, 1767–1776 (2003).
8. S. W. Spaulding, I. J. Chopra, R. S. Sherwin, S. S. Lyall, Effect of caloric restriction and dietary composition of serum T3 and reverse T3 in man. *J. Clin. Endocrinol. Metab.* **42**, 197–200 (1976).
9. J. L. Chan, K. Heist, A. M. DePaoli, J. D. Veldhuis, C. S. Mantzoros, The role of falling leptin levels in the neuroendocrine and metabolic adaptation to short-term starvation in healthy men. *J. Clin. Invest.* **111**, 1409–1421 (2003).
10. K. D. Burman *et al*., Nature of suppressed TSH secretion during undernutrition: Effect of fasting and refeeding on TSH responses to prolonged TRH infusions. *Metabolism* **29**, 46–52 (1980).
11. J. Unger, Fasting induces a decrease in serum thyroglobulin in normal subjects. *J. Clin. Endocrinol. Metab.* **67**, 1309–1311 (1988).
12. A. Boelen, W. M. Wiersinga, E. Fliers, Fasting-induced changes in the hypothalamus-pituitary-thyroid axis. *Thyroid* **18**, 123–129 (2008).
13. A. H. van der Spek, E. Fliers, A. Boelen, The classic pathways of thyroid hormone metabolism. *Mol. Cell. Endocrinol.* **458**, 29–38 (2017).
14. R. Mullur, Y. Y. Liu, G. A. Brent, Thyroid hormone regulation of metabolism. *Physiol. Rev.* **94**, 355–382 (2014).
15. H. K. Park, R. S. Ahima, Physiology of leptin: Energy homeostasis, neuroendocrine function and metabolism. *Metabolism* **64**, 24–34 (2015).
16. K. R. Vella *et al*., NPY and MC4R signaling regulate thyroid hormone levels during fasting through both central and peripheral pathways. *Cell Metab.* **14**, 780–790 (2011).
17. E. M. de Vries *et al*., Fasting-induced changes in hepatic thyroid hormone metabolism in male rats are independent of autonomic nervous input to the liver. *Endocrinology* **155**, 5033–5041 (2014).
18. C. Fekete *et al*., Agouti-related protein (AGRP) has a central inhibitory action on the hypothalamic-pituitary-thyroid (HPT) axis; Comparisons between the effect of AGRP and neuropeptide Y on energy homeostasis and the HPT axis. *Endocrinology* **143**, 3846–3853 (2002).
19. C. Fekete *et al*., Differential effects of central leptin, insulin, or glucose administration during fasting on the hypothalamic-pituitary-thyroid axis and feeding-related neurons in the arcuate nucleus. *Endocrinology* **147**, 520–529 (2006).
20. F. Guo, K. Bakal, Y. Minokoshi, A. N. Hollenberg, Leptin signaling targets the thyrotropin-releasing hormone gene promoter in vivo. *Endocrinology* **145**, 2221–2227 (2004).
21. M. A. da Veiga, Kde. J. Oliveira, F. H. Curty, C. C. de Moura, Thyroid hormones modulate the endocrine and autocrine/paracrine actions of leptin on thyrotropin secretion. *J. Endocrinol.* **183**, 243–247 (2004).
22. G. Legradi *et al*., Arcuate nucleus ablation prevents fasting-induced suppression of ProTRH mRNA in the hypothalamic paraventricular nucleus. *Neuroendocrinology* **68**, 89–97 (1998).
23. M. M. Poplawski, J. W. Mastaitis, X. J. Yang, C. V. Mobbs, Hypothalamic responses to fasting indicate metabolic reprogramming away from glycolysis toward lipid oxidation. *Endocrinology* **151**, 5206–5217 (2010).
24. Y. C. Tung *et al*., Novel leptin-regulated genes revealed by transcriptional profiling of the hypothalamic paraventricular nucleus. *J. Neurosci.* **28**, 12419–12426 (2008).

25. J. M. Rondeel *et al*., Effect of starvation and subsequent refeeding on thyroid function and release of hypothalamic thyrotropin-releasing hormone. *Neuroendocrinology* **56**, 348–353 (1992).
26. S. Diano, F. Naftolin, F. Goglia, T. L. Horvath, Fasting-induced increase in type II iodothyronine deiodinase activity and messenger ribonucleic acid levels is not reversed by thyroxine in the rat hypothalamus. *Endocrinology* **139**, 2879–2884 (1998).
27. K. N. Fontes *et al*., Differential regulation of thyroid hormone metabolism target genes during non-thyroidal [corrected] illness syndrome triggered by fasting or sepsis in adult mice. *Front. Physiol.* **8**, 828 (2017).
28. A. Boelen, J. Kwakkel, X. G. Vos, W. M. Wiersinga, E. Fliers, Differential effects of leptin and refeeding on the fasting-induced decrease of pituitary type 2 deiodinase and thyroid hormone receptor beta2 mRNA expression in mice. *J. Endocrinol.* **190**, 537–544 (2006).
29. E. D. Abel *et al*., Divergent roles for thyroid hormone receptor beta isoforms in the endocrine axis and auditory system. *J. Clin. Invest.* **104**, 291–300 (1999).
30. S. Minakhina *et al*., A direct comparison of thyroid hormone receptor protein levels in mice provides unexpected insights into thyroid hormone action. *Thyroid* **30**, 1193–1204 (2020).
31. F. E. Wondisford *et al*., Thyroid hormone inhibition of human thyrotropin beta-subunit gene expression is mediated by a cis-acting element located in the first exon. *J. Biol. Chem.* **264**, 14601–14604 (1989).
32. M. F. Langlois *et al*., A unique role of the beta-2 thyroid hormone receptor isoform in negative regulation by thyroid hormone. Mapping of a novel amino-terminal domain important for ligand-independent activation. *J. Biol. Chem.* **272**, 24927–24933 (1997).
33. J. D. Safer *et al*., Isoform variable action among thyroid hormone receptor mutants provides insight into pituitary resistance to thyroid hormone. *Mol. Endocrinol.* **11**, 16–26 (1997).
34. E. Compe *et al*., Dysregulation of the peroxisome proliferator-activated receptor target genes by XPD mutations. *Mol. Cell. Biol.* **25**, 6065–6076 (2005).
35. I. Iankova *et al*., Peroxisome proliferator-activated receptor gamma recruits the positive transcription elongation factor b complex to activate transcription and promote adipogenesis. *Mol. Endocrinol.* **20**, 1494–1505 (2006).
36. T. A. Knotts, R. S. Orkiszewski, R. G. Cook, D. P. Edwards, N. L. Weigel, Identification of a phosphorylation site in the hinge region of the human progesterone receptor and additional amino-terminal phosphorylation sites. *J. Biol. Chem.* **276**, 8475–8483 (2001).
37. D. Chen *et al*., Activation of estrogen receptor alpha by S118 phosphorylation involves a ligand-dependent interaction with TFIIH and participation of CDK7. *Mol. Cell* **6**, 127–137 (2000).
38. C. Rochette-Egly, S. Adam, M. Rossignol, J. M. Egly, P. Chambon, Stimulation of RAR alpha activation function AF-1 through binding to the general transcription factor TFIIH and phosphorylation by CDK7. *Cell* **90**, 97–107 (1997).
39. E. Gaillard *et al*., Phosphorylation by PKA potentiates retinoic acid receptor alpha activity by means of increasing interaction with and phosphorylation by cyclin H/cdk7. *Proc. Natl. Acad. Sci. U.S.A.* **103**, 9548–9553 (2006).
40. C. Glineur, M. Bailly, J. Ghysdael, The c-erbA alpha-encoded thyroid hormone receptor is phosphorylated in its amino terminal domain by casein kinase II. *Oncogene* **4**, 1247–1254 (1989).
41. M. K. Bhat, K. Ashizawa, S. Y. Cheng, Phosphorylation enhances the target gene sequence-dependent dimerization of thyroid hormone receptor with retinoid X receptor. *Proc. Natl. Acad. Sci. U.S.A.* **91**, 7927–7931 (1994).
42. D. Katz, M. J. Reginato, M. A. Lazar, Functional regulation of thyroid hormone receptor variant TR alpha 2 by phosphorylation. *Mol. Cell. Biol.* **15**, 2341–2348 (1995).
43. Y. T. Ting, S. Y. Cheng, Hormone-activated phosphorylation of human beta1 thyroid hormone nuclear receptor. *Thyroid* **7**, 463–469 (1997).
44. C. Tzagarakis-Foster, M. L. Privalsky, Phosphorylation of thyroid hormone receptors by protein kinase A regulates DNA recognition by specific inhibition of receptor monomer binding. *J. Biol. Chem.* **273**, 10926–10932 (1998).
45. P. J. Davis, A. Shih, H. Y. Lin, L. J. Martino, F. B. Davis, Thyroxine promotes association of mitogen-activated protein kinase and nuclear thyroid hormone receptor (TR) and causes serine phosphorylation of TR. *J. Biol. Chem.* **275**, 38032–38039 (2000).
46. C. M. Barbieri, A. M. Stock, Universally applicable methods for monitoring response regulator aspartate phosphorylation both in vitro and in vivo using Phos-tag-based reagents. *Anal. Biochem.* **376**, 73–82 (2008).
47. A. Dace *et al*., Hormone binding induces rapid proteasome-mediated degradation of thyroid hormone receptors. *Proc. Natl. Acad. Sci. U.S.A.* **97**, 8985–8990 (2000).
48. N. Shibusawa, A. N. Hollenberg, F. E. Wondisford, Thyroid hormone receptor DNA binding is required for both positive and negative gene regulation. *J. Biol. Chem.* **278**, 732–738 (2003).
49. K. R. Vella *et al*., Thyroid hormone signaling in vivo requires a balance between coactivators and corepressors. *Mol. Cell. Biol.* **34**, 1564–1575 (2014).
50. H. S. Camp, S. R. Tafuri, Regulation of peroxisome proliferator-activated receptor gamma activity by mitogen-activated protein kinase. *J. Biol. Chem.* **272**, 10811–10816 (1997).
51. H. S. Camp, S. R. Tafuri, T. Leff, c-Jun N-terminal kinase phosphorylates peroxisome proliferator-activated receptor-gamma1 and negatively regulates its transcriptional activity. *Endocrinology* **140**, 392–397 (1999).
52. A. S. Banks *et al*., An ERK/Cdk5 axis controls the diabetogenic actions of PPARγ. *Nature* **517**, 391–395 (2015).
53. N. Blom, T. Sicheritz-Pontén, R. Gupta, S. Gammeltoft, S. Brunak, Prediction of post-translational glycosylation and phosphorylation of proteins from the amino acid sequence. *Proteomics* **4**, 1633–1649 (2004).
54. K. Umesono, K. K. Murakami, C. C. Thompson, R. M. Evans, Direct repeats as selective response elements for the thyroid hormone, retinoic acid, and vitamin D3 receptors. *Cell* **65**, 1255–1266 (1991).
55. G. A. Brent *et al*., Capacity for cooperative binding of thyroid hormone (T3) receptor dimers defines wild type T3 response elements. *Mol. Endocrinol.* **6**, 502–514 (1992).
56. M. A. Lazar, T. J. Berrodin, H. P. Harding, Differential DNA binding by monomeric, homodimeric, and potentially heteromeric forms of the thyroid hormone receptor. *Mol. Cell. Biol.* **11**, 5005–5015 (1991).
57. E. M. de Vries *et al*., Regulation of type 3 deiodinase in rodent liver and adipose tissue during fasting. *Endocr. Connect.* **9**, 552–562 (2020).
58. R. S. Ahima *et al*., Role of leptin in the neuroendocrine response to fasting. *Nature* **382**, 250–252 (1996).
59. Y. Minokoshi *et al*., AMP-kinase regulates food intake by responding to hormonal and nutrient signals in the hypothalamus. *Nature* **428**, 569–574 (2004).
60. B. Kola, Role of AMP-activated protein kinase in the control of appetite. *J. Neuroendocrinol.* **20**, 942–951 (2008).
61. D. G. Hardie, B. E. Schaffer, A. Brunet, AMPK: An energy-sensing pathway with multiple inputs and outputs. *Trends Cell Biol.* **26**, 190–201 (2016).
62. C. Fekete, R. M. Lechan, Central regulation of hypothalamic-pituitary-thyroid axis under physiological and pathophysiological conditions. *Endocr. Rev.* **35**, 159–194 (2014).
63. M. López *et al*., Hypothalamic AMPK and fatty acid metabolism mediate thyroid regulation of energy balance. *Nat. Med.* **16**, 1001–1008 (2010).
64. D. Garcia, R. J. Shaw, AMPK: Mechanisms of cellular energy sensing and restoration of metabolic balance. *Mol. Cell* **66**, 789–800 (2017).
65. R. M. Abdulrahman *et al*., Impact of metformin and compound C on NIS expression and iodine uptake in vitro and in vivo: A role for CRE in AMPK modulation of thyroid function. *Thyroid* **24**, 78–87 (2014).
66. X. Meng, S. Xu, G. Chen, M. Derwahl, C. Liu, Metformin and thyroid disease. *J. Endocrinol.* **233**, R43–R51 (2017).
67. L. H. Duntas, J. Orgiazzi, G. Brabant, The interface between thyroid and diabetes mellitus. *Clin. Endocrinol. (Oxf.)* **75**, 1–9 (2011).
68. Y. Goldberg *et al*., Activation of protein kinase C or cAMP-dependent protein kinase increases phosphorylation of the c-erbA-encoded thyroid hormone receptor and of the v-erbA-encoded protein. *EMBO J.* **7**, 2425–2433 (1988).
69. D. Chen *et al*., Phosphorylation of human estrogen receptor alpha at serine 118 by two distinct signal transduction pathways revealed by phosphorylation-specific antisera. *Oncogene* **21**, 4921–4931 (2002).
70. R. Brunmeir, F. Xu, Functional regulation of PPARs through post-translational modifications. *Int. J. Mol. Sci.* **19**, 1738 (2018).
71. G. Barrera-Hernandez, K. S. Park, A. Dace, Q. Zhan, S. Y. Cheng, Thyroid hormone-induced cell proliferation in GC cells is mediated by changes in G1 cyclin/cyclin-dependent kinase levels and activity. *Endocrinology* **140**, 5267–5274 (1999).
72. J. D. Short *et al*., AMP-activated protein kinase signaling results in cytoplasmic sequestration of p27. *Cancer Res.* **68**, 6496–6506 (2008).
73. D. S. Machado *et al*., A thyroid hormone receptor mutation that dissociates thyroid hormone regulation of gene expression in vivo. *Proc. Natl. Acad. Sci. U.S.A.* **106**, 9441–9446 (2009).
74. P. Rajbhandari, M. S. Ozers, N. M. Solodin, C. L. Warren, E. T. Alarid, Peptidylprolyl isomerase pin1 directly enhances the DNA binding functions of estrogen receptor α. *J. Biol. Chem.* **290**, 13749–13762 (2015).
75. R. Narayanan, A. A. Adigun, D. P. Edwards, N. L. Weigel, Cyclin-dependent kinase activity is required for progesterone receptor function: Novel role for cyclin A/Cdk2 as a progesterone receptor coactivator. *Mol. Cell. Biol.* **25**, 264–277 (2005).
76. R. H. Wright *et al*., CDK2-dependent activation of PARP-1 is required for hormonal gene regulation in breast cancer cells. *Genes Dev.* **26**, 1972–1983 (2012).